



CHORUS

This is the accepted manuscript made available via CHORUS. The article has been published as:

Dissipation-assisted operator evolution method for capturing hydrodynamic transport

Tibor Rakovszky, C. W. von Keyserlingk, and Frank Pollmann

Phys. Rev. B **105**, 075131 — Published 16 February 2022

DOI: [10.1103/PhysRevB.105.075131](https://doi.org/10.1103/PhysRevB.105.075131)

Dissipation-assisted operator evolution method for capturing hydrodynamic transport

Tibor Rakovszky,¹ C.W. von Keyserlingk,² and Frank Pollmann^{1,3}

¹*Department of Physics, T42, Technische Universität München,
James-Frank-Straße 1, D-85748 Garching, Germany*

²*School of Physics & Astronomy, University of Birmingham, Birmingham, B15 2TT, UK*

³*Munich Center for Quantum Science and Technology (MCQST), Schellingstr. 4, D-80799 München, Germany*

We introduce the dissipation-assisted operator evolution (DAOE) method for calculating transport properties of strongly interacting lattice systems in the high temperature regime. DAOE is based on evolving observables in the Heisenberg picture, and applying an artificial dissipation acting on long operators. We represent the observable as a matrix product operator, and show that the dissipation leads to a decay of operator entanglement, allowing us to follow the dynamics to long times. We test this scheme by calculating spin and energy diffusion constants in a variety of physical models. By gradually weakening the dissipation, we are able to consistently extrapolate our results to the case of zero dissipation, thus estimating the physical diffusion constant with high precision.

Introduction.— Despite their complexity, thermalizing quantum many-body systems often exhibit universal hydrodynamical features in their low-frequency, long-wavelength limit [1–8]. Although these features are routinely measured in transport experiments, quantitatively connecting them to the underlying microscopic dynamics, e.g., deriving the transport coefficients from first principles, is notoriously difficult in practice [2, 9–13]. Established methods face an exponentially increasing cost, either with time or with system size, often leading to unreliable results [4, 14–17]. While methods have been proposed to circumvent these issues in certain cases [18–28], it remains unclear whether one can really overcome the exponential barrier for generic systems.

The purpose of this paper is to introduce a numerical method that tackles this problem and calculates transport properties from first principles in a controlled manner, while avoiding finite size and time restrictions. We achieve this by focusing on the Heisenberg picture dynamics of conserved densities. Motivated by recent results on operator spreading [29–32], we introduce an artificial dissipation that removes operators based on their ‘length’, which we define below. As a consequence, the time-evolved operator may be stored more compactly using standard tensor network techniques. The resulting dynamics depends on the specifics of the dissipative procedure, but in the limit of weak dissipation, the different methods all appear to converge. This allows us to estimate the physical result (here, a spin or energy diffusion constant) through extrapolation. Our results suggest that the simulation of transport in ergodic systems has a qualitatively smaller computational cost than solving the full many-body dynamical problem.

Numerical method.— We work with one-dimensional lattice models, labeling sites by $j = 1, \dots, L$. Consider the local density, q_j , of some conserved quantity $Q = \sum_j q_j$ (e.g., charge or energy). We are interested in dynamical correlations of these densities, $\langle q_i(0)q_j(t) \rangle_{\text{eq}}$, evaluated in some equilibrium state. We focus on infinite temperature, so that $\langle \dots \rangle_{\text{eq}} \equiv \text{Tr}[\dots]/\mathcal{N}$, with \mathcal{N}

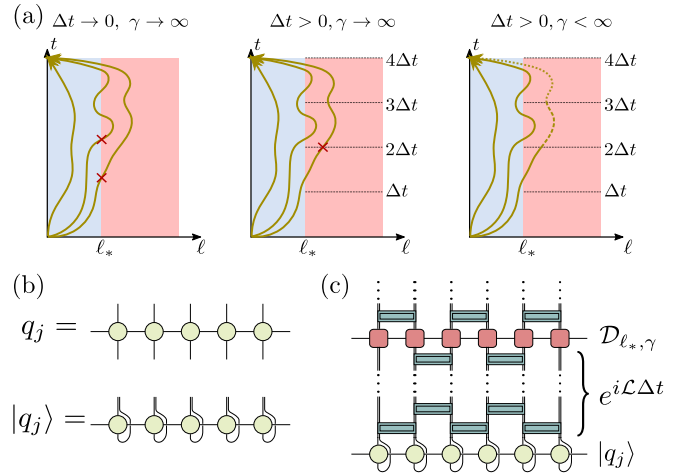


FIG. 1. Dissipation-assisted operator evolution (DAOE) method. (a) Sketch of the non-unitary evolution (2) as a sum over paths in operator space. For $\Delta t \rightarrow 0, \gamma \rightarrow \infty$, paths that leave the $\ell \leq \ell_*$ subspace are discarded immediately. Making Δt finite, we keep paths that wander off from this subspace but return before the next integer multiple of Δt . Finally, when $\Delta t, \gamma$ are both finite, all paths are kept, but the weight of those that spend time outside the ‘slow’ subspace is gradually reduced. (b): The operator (MPO) q_j can be reinterpreted as a state (MPS) $|q_j\rangle$ on a doubled Hilbert space. (c): One period of the DAOE as a tensor network. $|q_j\rangle$ is evolved with the TEBD algorithm up to time Δt . Then the dissipator $\mathcal{D}_{\ell_*, \gamma}$ is applied as a bond dimension $\ell_* + 1$ MPO.

the Hilbert space dimension. Here $q_j(t)$ is evolved unitarily in the Heisenberg picture, with a Hamiltonian H that conserves Q , $[H, Q] = 0$. Transport properties can be extracted from such correlations, as we detail below.

In what follows, we shall find it useful to think of operators as vectors in an enlarged Hilbert space of size \mathcal{N}^2 . In a matrix product operator (MPO) representation, this is equivalent to combining the two physical legs into a single leg, turning it into a matrix product state (MPS), as illustrated by Fig. 1(b). We use the notation $|q_j\rangle$ for the ‘vectorized’ operator, and introduce

an inner product on this space as $\langle A|B\rangle \equiv \langle A^\dagger B\rangle_{\text{eq}}$. The Heisenberg equation of motion can be rewritten as $\partial_t|q_j\rangle = i[H, q_j] \equiv i\mathcal{L}|q_j\rangle$, which defines the *Liouvillian* superoperator, \mathcal{L} . This is solved by $|q_j(t)\rangle = e^{i\mathcal{L}t}|q_j\rangle$. Importantly, we are only interested in the matrix elements of $e^{i\mathcal{L}t}$ in the ‘slow’ subspace, spanned by the conserved densities: $\langle q_i|e^{i\mathcal{L}t}|q_j\rangle = \langle q_i q_j(t)\rangle_{\text{eq}}$. This *projected* evolution is generically no longer unitary.

We wish to approximate this non-unitary evolution by gradually taking into account the effect of the ‘bath’, meaning all the remaining operators that we are not projecting onto. We will do this in a more general way, where we include not only conserved densities, but all sufficiently local operators in the slow subspace. To be concrete, let us imagine a spin-1/2 chain. Then a basis of all 4^L operators is given by *Pauli strings*, products of the four Pauli matrices $\mathbb{1}, X, Y, Z$. To each Pauli string \mathcal{S} , we can associate a *length* $\ell_{\mathcal{S}}$, which is simply the number of non-trivial Paulis occurring in it. For example, $\mathbb{1}, X_j, Z_i Y_j$ have lengths $\ell = 0, 1, 2$, respectively. We can then define a *dissipation superoperator* that decreases the weight of all strings longer than some cutoff length ℓ_* as

$$\mathcal{D}_{\ell_*, \gamma}[\mathcal{S}] = \begin{cases} \mathcal{S} & \text{if } \ell_{\mathcal{S}} \leq \ell_* \\ e^{-\gamma(\ell_{\mathcal{S}} - \ell_*)} \mathcal{S} & \text{otherwise.} \end{cases} \quad (1)$$

The cutoff length ℓ_* is introduced to ensure that the physically most relevant operators, such as conserved densities, are not affected by the dissipator.

We are now in a position to describe our proposed method. We define a modified time evolution, by applying the dissipator with period Δt . That is, for time $t \in [N, N+1)\Delta t$ (for $N \in \mathbb{N}$), we consider the time evolved local density defined by

$$|\tilde{q}_j(t)\rangle = e^{i\mathcal{L}(t-N\Delta t)} (\mathcal{D}_{\ell_*, \gamma} e^{i\mathcal{L}\Delta t})^N |q_j\rangle; \quad (2)$$

we dub this *dissipation-assisted operator evolution* (DAOE). Eq. (2) is clearly very different from the true, unitarily evolved operator $|q_j(t)\rangle$. However, we propose that the dissipative evolution can be made to correctly capture the correlations with other slow operators, particularly conserved densities, $\langle q_i|\tilde{q}_j(t)\rangle \approx \langle q_i|q_j(t)\rangle$.

Intuitively, Δt and $1/\gamma$ both play a similar role, limiting the amount of time an operator is allowed to spend outside the $\ell \leq \ell_*$ subspace. While at $\Delta t \rightarrow 0$, $\gamma \rightarrow \infty$ the dynamics is projected down to this subspace [33], making either Δt or γ finite allows the operators to go outside, but only for a limited amount of time (in fact, when γ is small, results depend on the ratio $\gamma/\Delta t$ only [34]). One can think of this as summing up certain contributions in a path-integral representation of the propagator $\langle q_i|e^{i\mathcal{L}t}|q_j\rangle$, as illustrated in Fig. 1(a). Unitary evolution is recovered by taking either $\gamma \rightarrow 0$, $\Delta t \rightarrow \infty$ or $\ell_* \rightarrow \infty$. In practice, we shall find it most useful to take the first option, keeping ℓ_* and Δt fixed

while approaching the unitary limit through decreasing γ . The spirit of this approximation is closely related to the well-known *memory matrix formalism* [2, 9–12, 35–38], with the ‘short’ ($\ell \leq \ell_*$) and ‘long’ ($\ell > \ell_*$) operators playing the role of the ‘slow’ and ‘fast’ subspaces, and Δt and γ providing a cutoff for the memory time

The correlators considered are affected by the dissipation through ‘backflow’ processes [31], wherein a long Pauli string in $q_j(t')$ at time $t' < t$ develops a component on a short operator, such as q_i , by time t . DAOE relies on the assumption that such backflow is weak in generic systems, which we expect to hold for two reasons. First, simple entropic arguments show that operators are more likely to grow in size than to shrink. Second, the many different backflow paths are expected to come with effectively random phases, leading to destructive interference. In the absence of conservation laws, one can easily argue that these lead to backflow effects being exponentially suppressed in ℓ_* . With conservation laws, the situation is more complicated [31, 32]. The largest contribution is expected from cases when q_i evolves into a product of several densities, $q_{i_1} \dots q_{i_\ell}$, and then back. Such products are ‘slow’ operators and have significant components that fail to grow ballistically. Nevertheless, we posit that these processes are still suppressed exponentially in ℓ . A key insight is that the decays of the densities multiply together, resulting in a behavior $\sim t^{-\ell/2}$, with ℓ appearing in the exponent. A detailed analysis of backflow processes, supporting this conclusion, is provided in Ref. 39.

To reap the benefits of the dissipation, we represent $|\tilde{q}_j(t)\rangle$ as an MPS. The unitary part of the evolution can then be done with standard MPS techniques; for the nearest-neighbor Hamiltonians studied below, the time-evolving block decimation (TEBD) algorithm [15, 16, 40, 41] provides an efficient solution. In this language, the superoperator $\mathcal{D}_{\ell_*, \gamma}$ becomes a matrix product operator (MPO) [15, 41, 42]. One can then straightforwardly evaluate Eq. (2), as illustrated in Fig. 1(c). As we will show, this can be done accurately with relatively low bond dimension, even for large systems and long times, provided that the dissipation is sufficiently strong.

$\mathcal{D}_{\ell_*, \gamma}$ in fact has an exact MPO representation with bond dimension $\ell_* + 1$. We label the local basis ‘states’ by $n = \mathbb{1}, X, Y, Z$ (generalization to higher spin is straightforward). We then write the local MPO tensor, $W_{ab}^{nn'}$, as a matrix acting on the virtual indices $a, b = 0, 1, \dots, \ell_*$. They read $W_{ab}^{\mathbb{1}\mathbb{1}} = \delta_{a=b}$ and $W_{ab}^{XX} = W_{ab}^{YY} = W_{ab}^{ZZ} = \delta_{a=b-1} + e^{-\gamma} \delta_{a=b=\ell_*}$, all others being zero. The MPO is contracted with the vector $v_L = (1, 0, \dots, 0)$ on the left, and $v_R = (1, \dots, 1, 1)$ on the right. It is easy to check that this reproduces the desired result.

The main limitation in the MPS representation of $|\tilde{q}_j\rangle$ is the *operator entanglement* [43–48], $S_{\text{vN}}[|\tilde{q}_j(t)\rangle]$, defined as the half-chain von Neumann entropy of the normalized state $|\tilde{q}_j(t)\rangle/\sqrt{\langle \tilde{q}_j(t)|\tilde{q}_j(t)\rangle}$. For generic unitary dynam-

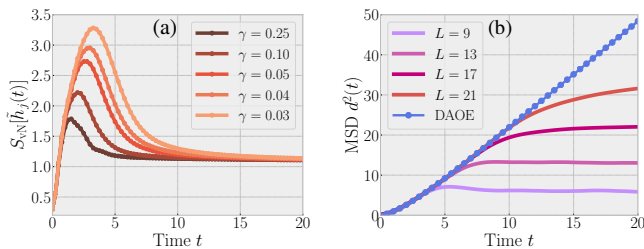


FIG. 2. Testing DAOE on the Ising model (4). (a) shows how the dissipation (for $\ell_* = 2$, $\Delta t = 0.25$) suppresses operator entanglement (measured in units of $\ln 2$). (b) shows that the MSD (3) is correctly captured to long times by the DAOE (same ℓ_* , Δt ; $\gamma = 0.03$, using bond dimensions $\chi = 512$), by comparing to exact results on small chains ($L = 9, 13, 17, 21$).

ics, it tends to increase linearly [49, 50], $S_{\text{vN}}[q_j(t)] \propto t$. In this case, the bond dimension χ needed for a faithful MPO/MPS representation grows exponentially with t , cutting short the times one can simulate [15, 16]. We find that applying the dissipator *decreases* the operator entanglement, and this effect always becomes dominant at long times (see Fig. 2(a)); a similar effect was noted very recently in another context in Ref. 51. This key observation means that we can calculate $|\tilde{q}_j(t)\rangle$ with high precision, up to very long times, with a *finite* χ .

Results. — We use our method to calculate the dynamical correlations between the central site $i = \frac{L+1}{2}$ (we take L odd) and all other positions, $C_j(t) \equiv \text{Tr}[q_j \tilde{q}_{\frac{L+1}{2}}(t)]/\mathcal{N}$. We normalize these such that $\sum_j C_j(0) = 1$. One can characterize the spreading of correlations by the *mean-square displacement* (MSD),

$$d^2(t) \equiv \sum_j C_j(t) j^2 - \left(\sum_j C_j(t) j \right)^2. \quad (3)$$

In the strongly interacting, non-integrable systems we study, high-temperature transport of conserved quantities is expected to be *diffusive* [2, 3, 52, 53], which manifests in a linear growth of the MSD at long times, $d^2(t) \propto t$. This suggests defining a *time-dependent diffusion constant* [4, 54–57] as $2D(t) \equiv \partial_t d^2(t)$. The physical diffusion constant is then $D \equiv \lim_{t \rightarrow \infty} D(t)$ (assuming $L \rightarrow \infty$ first). Further information about the frequency- and wavevector-dependence of the conductivity can be obtained by looking at space-time dependence of $C_j(t)$ [4, 6, 58].

Our approach is as follows. We calculate $D(t)$ for the dissipative evolution, and then approach the unitary dynamics by decreasing γ , while keeping Δt and ℓ_* fixed. We decrease γ until we observe signs of convergence, allowing us to extrapolate the results for D back to $\gamma \rightarrow 0$. We can estimate the accuracy of this extrapolation by comparing different values of ℓ_* . As stated above, the value of Δt is in principle irrelevant, as one finds a scaling collapse as a function of $\gamma/\Delta t$ for small γ . However,

in practice, Δt should be small enough so that one can follow the full dynamics up to Δt with the given bond dimension. It is also numerically more efficient not to make Δt too small, in order to reduce the number of MPO-to-MPS multiplications we need to perform. We find that $\Delta t \approx 1$ (in units of microscopic couplings) works well. We investigate two Hamiltonians which we expect to be generic; further results on discrete circuit models are presented in [34].

Energy transport in the Ising chain. We first consider the Ising model in a tilted field,

$$H = \sum_j h_j \equiv \sum_j \left(g_x X_j + g_z Z_j + \frac{Z_{j-1} Z_j + Z_j Z_{j+1}}{2} \right). \quad (4)$$

We fix $g_x = 1.4$ and $g_z = 0.9045$. At these values, we expect the model to be strongly chaotic [59, 60], and hard to simulate exactly, due to fast entanglement growth. Here, h_j is the energy associated to site j . This is the only local conserved density in the model, and its correlations capture energy (or heat) transport [60]. We therefore take $q_j \equiv h_j$ in this case, and evolve $h_{\frac{L+1}{2}}$, as an MPO, according to Eq. (2). We perform the unitary part of the dynamics with TEBD, using a small Trotter time-step 0.01. We take large enough systems ($L = 51$) such that finite size effects are negligible at the times we study.

Fig. 2(a) confirms that the dissipation limits the operator entanglement growth, so that the entropy $S_{\text{vN}}[h_j(t)]$ peaks and then decreases. The time and height of the peak increase as γ gets smaller, but for any non-zero γ , dissipation dominates at long times. Moreover, we find that after the peak, S_{vN} approaches 1 in units of $\ln 2$, indicating that the operator is increasingly dominated by the local densities, $h_{\frac{L+1}{2}}(t) \approx \sum_j C_j(t) h_j$.

We benchmark our method by comparing it to exact results on small systems, calculated using the *canonical typicality* approach [14, 61, 62], for up to $L = 21$ sites. In this case, finite-size effects limit the times one can reach to $t \approx 10$. We compare these to the dissipative method for a particular set of parameters, $\ell_* = 2, \Delta t = 0.25, \gamma = 0.03$, which we expect to be close to being converged to the physical diffusion constant (see below). The results for the MSD are presented in Fig. 2(b). The curve from the dissipative evolution follows the exact results, and then continues to grow linearly to much longer times, well beyond the reach of exact numerics. This is despite the fact that at these times, the dissipation already had a large effect (as measured, for example, by the decay of S_{vN}), and $h_{\frac{L+1}{2}}(t)$ is far from the true time-evolved operator. Note that the dissipation is essential in allowing us to reach long times; for the same bond dimension ($\chi = 512$), TEBD without dissipation starts deviating from the exact results around times $t \approx 7 - 8$ due to truncation errors.

Having established the potential of the DAOE method,

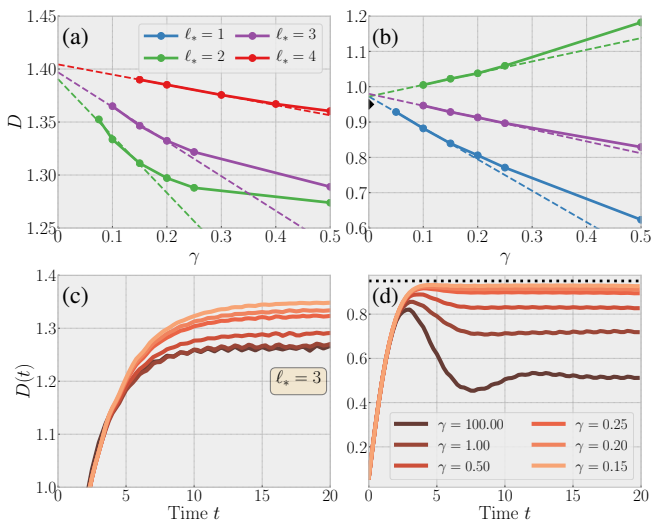


FIG. 3. Estimating the diffusion constant. (a,c) show data for the Ising chain (4) and (b,d) for the XX ladder (5). We fix $\Delta t = 1$ and use bond dimensions up to $\chi = 768$. In (c) and (d) we show results for the time-dependent diffusion constant at a fixed $\ell_* = 3$ for varying γ , showing clear signs of convergence. In (a,b) we show the estimate for D (taken as the average of $D(t)$ in the interval $t \in [15, 20]$). Data for the weakest dissipations is well fit by a linear extrapolation, and results for different ℓ_* give consistent estimates for the physical diffusion constant. In (b) and (d), the \blacktriangleright and dotted line represent the estimate $D = 0.95$ from Ref. 63.

we now embark on the strategy outlined above, approaching the unitary limit by decreasing γ gradually from $\gamma = \infty$. For each set of parameters, we calculate a time-dependent diffusion constant $D_{\ell_*, \Delta t}(t; \gamma)$. In the limit $\gamma \rightarrow 0$ one would recover the physical result, $\lim_{\gamma \rightarrow 0} D_{\ell_*, \Delta t}(t; \gamma) = D(t)$, for any ℓ_* and Δt . In practice, we are limited to some minimal γ we can simulate with a certain bond dimension, while avoiding truncation errors. However, as we show, one can extrapolate from the data to get an estimate for the diffusion constant at $\gamma = 0$. Estimates for different ℓ_* then allow us to check the accuracy of this extrapolation.

The results are shown in Fig. 3(a,c), for $\Delta t = 1$ and $\ell_* = 2, 3, 4$. $D(t)$ saturates to a γ -dependent constant. When γ is made sufficiently small, we find that the results converge. The last few data points are well fitted by a straight line, which allows us to extrapolate D back to $\gamma = 0$. The extrapolated results for different choices of ℓ_* all agree to within $\approx 1\%$ error, supporting our conclusions that we indeed reached the physical diffusion constant (in this case, $D \approx 1.40$). This constitutes strong evidence that our method can successfully capture transport coefficients to a high precision.

Spin transport in the XX ladder. Next, we study a spin-1/2 model on a two-leg ladder. We denote by $j = 1, \dots, L$ the rungs of the ladder, and use $a = 1, 2$ for the two legs. Pauli operators on a given site are specified as

$X_{j,a}$, etc. The Hamiltonian then reads

$$H = \sum_{j=1}^L \sum_{a=1,2} (X_{j,a} X_{j+1,a} + Y_{j,a} Y_{j+1,a}) + \sum_{j=1}^L (X_{j,1} X_{j,2} + Y_{j,1} Y_{j,2}). \quad (5)$$

Besides energy, this model also conserves the spin z component, $\sum_{j,a} Z_{j,a}$. We examine the transport of the corresponding local conserved density $q_j = Z_j \equiv (Z_{j,1} + Z_{j,2})/2$ along the chain. We take a system of $L = 41$ rungs, which is large enough to avoid finite-size effects, up to the times ($t \approx 20$) that we simulate.

Spin transport in this model has been studied in a number of previous works, finding clear evidence of diffusive behavior with a diffusion constant $D \approx 0.95$ [23, 63, 64]. Here we show that our method reproduces this result on much larger systems. We perform the same analysis as in the Ising model, comparing D for different γ and extrapolating back to $\gamma = 0$; the results are shown in Fig. 3(b,d). We find that the extrapolated results are all within the range $D \approx 0.96 - 0.98$ (even for $\ell_* = 1$, where energy-conservation is violated). The fact that these values are all very close to one another, and to the previous result, strongly supports the validity of our method.

Conclusions.— We introduced a controlled numerical method for computing transport properties in strongly interacting quantum systems at high temperatures. Our method is based on neglecting ‘backflow’ from complicated to simple operators. We provided a simple implementation of this method, using matrix product states, which allowed us to calculate dynamical correlations without finite-size or finite-time limitations. We demonstrated the utility of this approach on two spin models, showing that it can be used to estimate diffusion constants with high precision. An interesting open question is whether the method could be further improved by using ideas from Refs. 24, 27, and 65.

There are a variety of physical problems that would be interesting to explore with this method, such as transport in 1D quantum magnets [66–69], disordered models [70–74] or long-range interacting [75] systems, where existing methods are even more limited. There might also be applications in quantum chemistry, where tensor network methods are becoming increasingly important [76–80]. A natural extension of our method is to finite temperatures. We expect it to work well at high temperatures, where the thermal density matrix is dominated by short operators [81–86], while it presumably breaks down as the low-temperature limit is approached. Precisely when and how this happens is itself an interesting question.

Acknowledgements.—The authors thank David Huse, Philipp Dumitrescu, Tarun Grover, Andrew Green, Fabian Heidrich-Meisner, Sean Hartnoll, Vedika Khemani, Minki Jeong, Xiangyu Cao and Daniel Parker for

stimulating discussions, and in particular Ehud Altman for his talk at the KITP Conference “Novel Approaches to Quantum Dynamics” that in part inspired our work. CvK is supported by a Birmingham Fellowship. FP is funded by the European Research Council (ERC) under the European Unions Horizon 2020 research and innovation program (grant agreement No. 771537). FP acknowledges the support of the DFG Research Unit FOR 1807 through grants no. PO 1370/2-1, TRR80, and the Deutsche Forschungsgemeinschaft (DFG, German Research Foundation) under Germany’s Excellence Strategy EXC-2111-390814868. This work was initiated at KITP where TR, CvK, and FP were supported in part by the National Science Foundation under Grant No. NSF PHY-1748958 (KITP) during the “Dynamics of Quantum Information” program. TR further acknowledges the hospitality of KITP as part of the graduate fellowship program of the Fall of 2019, during which some of this work was performed.

-
- [1] Paul M Chaikin and Tom C Lubensky, *Principles of condensed matter physics*, Vol. 10 (Cambridge university press Cambridge, 1995).
- [2] Dieter Forster, *Hydrodynamic fluctuations, broken symmetry, and correlation functions* (CRC Press, 2018).
- [3] Leo P Kadanoff and Paul C Martin, “Hydrodynamic equations and correlation functions,” *Annals of Physics* **24**, 419 – 469 (1963).
- [4] B. Bertini, F. Heidrich-Meisner, C. Karrasch, T. Prosen, R. Steinigeweg, and M. Žnidarič, “Finite-temperature transport in one-dimensional quantum lattice models,” (2020), [arXiv:2003.03334](https://arxiv.org/abs/2003.03334).
- [5] Hong Liu and Paolo Glorioso, “Lectures on non-equilibrium effective field theories and fluctuating hydrodynamics,” in *Proceedings of Theoretical Advanced Study Institute Summer School 2017 “Physics at the Fundamental Frontier” — PoS(TASI2017)* (Sissa Medialab, 2018).
- [6] Xinyi Chen-Lin, Luca V. Delacrétaz, and Sean A. Hartnoll, “Theory of diffusive fluctuations,” *Phys. Rev. Lett.* **122**, 091602 (2019).
- [7] Benjamin Doyon, “Lecture notes on generalised hydrodynamics,” (2019), [arXiv:1912.08496](https://arxiv.org/abs/1912.08496).
- [8] Jonathan Lux, Jan Müller, Aditi Mitra, and Achim Rosch, “Hydrodynamic long-time tails after a quantum quench,” *Phys. Rev. A* **89**, 053608 (2014).
- [9] Y Pomeau and P Résibois, “Time dependent correlation functions and mode-mode coupling theories,” *Physics Reports* **19**, 63 – 139 (1975).
- [10] J. Rau and B. Müller, “From reversible quantum microdynamics to irreversible quantum transport,” *Physics Reports* **272**, 1 – 59 (1996).
- [11] Robert Zwanzig, *Nonequilibrium statistical mechanics* (Oxford University Press, 2001).
- [12] Hermann Grabert, *Projection Operator Techniques in Nonequilibrium Statistical Mechanics* (Springer Berlin Heidelberg, 1982).
- [13] Tom Banks and Andrew Lucas, “Emergent entropy production and hydrodynamics in quantum many-body systems,” *Phys. Rev. E* **99**, 022105 (2019).
- [14] Tjark Heitmann, Jonas Richter, Dennis Schubert, and Robin Steinigeweg, “Selected applications of typicality to real-time dynamics of quantum many-body systems,” (2020), [arXiv:2001.05289](https://arxiv.org/abs/2001.05289).
- [15] Ulrich Schollwöck, “The density-matrix renormalization group in the age of matrix product states,” *Annals of Physics* **326**, 96 – 192 (2011), january 2011 Special Issue.
- [16] Sebastian Paeckel, Thomas Köhler, Andreas Swoboda, Salvatore R. Manmana, Ulrich Schollwöck, and Claudius Hubig, “Time-evolution methods for matrix-product states,” *Annals of Physics* **411**, 167998 (2019).
- [17] V. S. Viswanath and Gerhard Müller, *The Recursion Method* (Springer Berlin Heidelberg, 1994).
- [18] Tomaž Prosen and Marko Žnidarič, “Matrix product simulations of non-equilibrium steady states of quantum spin chains,” *Journal of Statistical Mechanics: Theory and Experiment* **2009**, P02035 (2009).
- [19] Marko Žnidarič, “Nonequilibrium steady-state kubo formula: Equality of transport coefficients,” *Phys. Rev. B* **99**, 035143 (2019).
- [20] Jutho Haegeman, J. Ignacio Cirac, Tobias J. Osborne, Iztok Pižorn, Henri Verschelde, and Frank Verstraete, “Time-dependent variational principle for quantum lattices,” *Phys. Rev. Lett.* **107**, 070601 (2011).
- [21] Jutho Haegeman, Christian Lubich, Ivan Oseledets, Bart Vandereycken, and Frank Verstraete, “Unifying time evolution and optimization with matrix product states,” *Phys. Rev. B* **94**, 165116 (2016).
- [22] Eyal Leviatan, Frank Pollmann, Jens H. Bardarson, David A. Huse, and Ehud Altman, “Quantum thermalization dynamics with matrix-product states,” (2017), [arXiv:1702.08894](https://arxiv.org/abs/1702.08894).
- [23] Benedikt Kloss, Yevgeny Bar Lev, and David Reichman, “Time-dependent variational principle in matrix-product state manifolds: Pitfalls and potential,” *Phys. Rev. B* **97**, 024307 (2018).
- [24] Christopher David White, Michael Zaletel, Roger S. K. Mong, and Gil Refael, “Quantum dynamics of thermalizing systems,” *Phys. Rev. B* **97**, 035127 (2018).
- [25] Jonathan Wurtz, Anatoli Polkovnikov, and Dries Sels, “Cluster truncated wigner approximation in strongly interacting systems,” *Annals of Physics* **395**, 341 – 365 (2018).
- [26] C. Krumnow, J. Eisert, and Ö. Legeza, “Towards overcoming the entanglement barrier when simulating long-time evolution,” (2019), [arXiv:1904.11999](https://arxiv.org/abs/1904.11999).
- [27] Daniel E. Parker, Xiangyu Cao, Alexander Avdoshkin, Thomas Scaffidi, and Ehud Altman, “A universal operator growth hypothesis,” *Phys. Rev. X* **9**, 041017 (2019).
- [28] A. Hallam, J. G. Morley, and A. G. Green, “The lyapunov spectra of quantum thermalisation,” *Nature Communications* **10** (2019), 10.1038/s41467-019-10336-4.
- [29] Adam Nahum, Sagar Vijay, and Jeongwan Haah, “Operator spreading in random unitary circuits,” *Phys. Rev. X* **8**, 021014 (2018).
- [30] C. W. von Keyserlingk, Tibor Rakovszky, Frank Pollmann, and S. L. Sondhi, “Operator hydrodynamics, otocs, and entanglement growth in systems without conservation laws,” *Phys. Rev. X* **8**, 021013 (2018).
- [31] Vedika Khemani, Ashvin Vishwanath, and David A. Huse, “Operator spreading and the emergence of dissi-

- passive hydrodynamics under unitary evolution with conservation laws,” *Phys. Rev. X* **8**, 031057 (2018).
- [32] Tibor Rakovszky, Frank Pollmann, and C. W. von Keyserlingk, “Diffusive hydrodynamics of out-of-time-ordered correlators with charge conservation,” *Phys. Rev. X* **8**, 031058 (2018).
- [33] Approximations of this sort have appeared in other contexts [87–89].
- [34] See online supplemental material for details.
- [35] Robert Zwanzig, “Memory effects in irreversible thermodynamics,” *Phys. Rev.* **124**, 983–992 (1961).
- [36] Hazime Mori, “Transport, collective motion, and brownian motion,” *Progress of Theoretical Physics* **33**, 423–455 (1965).
- [37] P. Jung, R. W. Helmes, and A. Rosch, “Transport in almost integrable models: Perturbed heisenberg chains,” *Phys. Rev. Lett.* **96**, 067202 (2006).
- [38] Peter Jung and Achim Rosch, “Lower bounds for the conductivities of correlated quantum systems,” *Phys. Rev. B* **75**, 245104 (2007).
- [39] C. W. von Keyserlingk, Frank Pollmann, and Tibor Rakovszky, “Operator backflow and the classical simulation of quantum transport,” (2021), [arXiv:2111.09904](https://arxiv.org/abs/2111.09904).
- [40] Guifré Vidal, “Efficient classical simulation of slightly entangled quantum computations,” *Phys. Rev. Lett.* **91**, 147902 (2003).
- [41] F. Verstraete, V. Murg, and J.I. Cirac, “Matrix product states, projected entangled pair states, and variational renormalization group methods for quantum spin systems,” *Advances in Physics* **57**, 143–224 (2008), <https://doi.org/10.1080/14789940801912366>.
- [42] B Pirvu, V Murg, J I Cirac, and F Verstraete, “Matrix product operator representations,” *New Journal of Physics* **12**, 025012 (2010).
- [43] Paolo Zanardi, “Entanglement of quantum evolutions,” *Phys. Rev. A* **63**, 040304 (2001).
- [44] Jayendra N. Bandyopadhyay and Arul Lakshminarayanan, “Entangling power of quantum chaotic evolutions via operator entanglement,” (2005), [arXiv:quant-ph/0504052](https://arxiv.org/abs/quant-ph/0504052).
- [45] Tomaž Prosen and Iztok Pižorn, “Operator space entanglement entropy in a transverse ising chain,” *Phys. Rev. A* **76**, 032316 (2007).
- [46] Iztok Pižorn and Tomaž Prosen, “Operator space entanglement entropy in xy spin chains,” *Phys. Rev. B* **79**, 184416 (2009).
- [47] J Dubail, “Entanglement scaling of operators: a conformal field theory approach, with a glimpse of simulability of long-time dynamics in 1+1d,” *Journal of Physics A: Mathematical and Theoretical* **50**, 234001 (2017).
- [48] Tianci Zhou and David J. Luitz, “Operator entanglement entropy of the time evolution operator in chaotic systems,” *Phys. Rev. B* **95**, 094206 (2017).
- [49] Tomaž Prosen and Marko Žnidarič, “Is the efficiency of classical simulations of quantum dynamics related to integrability?” *Phys. Rev. E* **75**, 015202 (2007).
- [50] Cheryne Jonay, David A. Huse, and Adam Nahum, “Coarse-grained dynamics of operator and state entanglement,” (2018), [arXiv:1803.00089](https://arxiv.org/abs/1803.00089).
- [51] Kyungjoo Noh, Liang Jiang, and Bill Fefferman, “Efficient classical simulation of noisy random quantum circuits in one dimension,” (2020), [arXiv:2003.13163](https://arxiv.org/abs/2003.13163).
- [52] N. Bloembergen, “On the interaction of nuclear spins in a crystalline lattice,” *Physica* **15**, 386 – 426 (1949).
- [53] P.G. De Gennes, “Inelastic magnetic scattering of neutrons at high temperatures,” *Journal of Physics and Chemistry of Solids* **4**, 223 – 226 (1958).
- [54] R. Steinigeweg, H. Wichterich, and J. Gemmer, “Density dynamics from current auto-correlations at finite time- and length-scales,” *EPL (Europhysics Letters)* **88**, 10004 (2009).
- [55] R. Steinigeweg, F. Jin, D. Schmidtke, H. De Raedt, K. Michielsen, and J. Gemmer, “Real-time broadening of nonequilibrium density profiles and the role of the specific initial-state realization,” *Phys. Rev. B* **95**, 035155 (2017).
- [56] Yonghong Yan, Feng Jiang, and Hui Zhao, “Energy spread and current-current correlation in quantum systems,” *The European Physical Journal B* **88** (2015), [10.1140/epjb/e2014-50797-4](https://doi.org/10.1140/epjb/e2014-50797-4).
- [57] David J. Luitz and Yevgeny Bar Lev, “The ergodic side of the many-body localization transition,” *Annalen der Physik* **529**, 1600350 (2017).
- [58] Henk van Beijeren, “Transport properties of stochastic lorentz models,” *Rev. Mod. Phys.* **54**, 195–234 (1982).
- [59] J. Karthik, Auditya Sharma, and Arul Lakshminarayanan, “Entanglement, avoided crossings, and quantum chaos in an ising model with a tilted magnetic field,” *Phys. Rev. A* **75**, 022304 (2007).
- [60] Hyungwon Kim and David A. Huse, “Ballistic spreading of entanglement in a diffusive nonintegrable system,” *Phys. Rev. Lett.* **111**, 127205 (2013).
- [61] Robin Steinigeweg, Jochen Gemmer, and Wolfram Brenig, “Spin-current autocorrelations from single pure-state propagation,” *Phys. Rev. Lett.* **112**, 120601 (2014).
- [62] Robin Steinigeweg, Jochen Gemmer, and Wolfram Brenig, “Spin and energy currents in integrable and non-integrable spin- $\frac{1}{2}$ chains: A typicality approach to real-time autocorrelations,” *Phys. Rev. B* **91**, 104404 (2015).
- [63] R. Steinigeweg, F. Heidrich-Meisner, J. Gemmer, K. Michielsen, and H. De Raedt, “Scaling of diffusion constants in the spin- $\frac{1}{2}$ xx ladder,” *Phys. Rev. B* **90**, 094417 (2014).
- [64] C. Karrasch, D. M. Kennes, and F. Heidrich-Meisner, “Spin and thermal conductivity of quantum spin chains and ladders,” *Phys. Rev. B* **91**, 115130 (2015).
- [65] Christian B. Mendl, “Time evolution of matrix product operators with energy conservation,” (2018), [arXiv:1812.11876](https://arxiv.org/abs/1812.11876).
- [66] Marko Ljubotina, Marko Žnidarič, and Tomaž Prosen, “Spin diffusion from an inhomogeneous quench in an integrable system,” *Nature communications* **8**, 1–6 (2017).
- [67] Jacopo De Nardis, Marko Medenjak, Christoph Karrasch, and Enej Ilievski, “Universality classes of spin transport in one-dimensional isotropic magnets: the onset of logarithmic anomalies,” (2020), [arXiv:2001.06432](https://arxiv.org/abs/2001.06432) [[cond-mat.stat-mech](https://arxiv.org/abs/2001.06432)].
- [68] Maxime Dupont and Joel E. Moore, “Universal spin dynamics in infinite-temperature one-dimensional quantum magnets,” *Phys. Rev. B* **101**, 121106 (2020).
- [69] F. Xiao, J. S. Möller, T. Lancaster, R. C. Williams, F. L. Pratt, S. J. Blundell, D. Ceresoli, A. M. Barton, and J. L. Manson, “Spin diffusion in the low-dimensional molecular quantum heisenberg antiferromagnet $\text{Cu}(\text{pyz})(\text{NO}_3)_2$ detected with implanted muons,” *Phys. Rev. B* **91**, 144417 (2015).
- [70] Kartiek Agarwal, Sarang Gopalakrishnan, Michael Knap, Markus Müller, and Eugene Demler, “Anomalous diffusion and griffiths effects near the many-body localization

- transition,” *Phys. Rev. Lett.* **114**, 160401 (2015).
- [71] Yevgeny Bar Lev, Guy Cohen, and David R. Reichman, “Absence of diffusion in an interacting system of spinless fermions on a one-dimensional disordered lattice,” *Phys. Rev. Lett.* **114**, 100601 (2015).
- [72] Andrew C. Potter, Romain Vasseur, and S. A. Parameswaran, “Universal properties of many-body delocalization transitions,” *Phys. Rev. X* **5**, 031033 (2015).
- [73] Ronen Vosk, David A. Huse, and Ehud Altman, “Theory of the many-body localization transition in one-dimensional systems,” *Phys. Rev. X* **5**, 031032 (2015).
- [74] Marko Žnidarič, Antonello Scardicchio, and Vipin Kerala Varma, “Diffusive and subdiffusive spin transport in the ergodic phase of a many-body localizable system,” *Phys. Rev. Lett.* **117**, 040601 (2016).
- [75] Alexander Schuckert, Izabella Lovas, and Michael Knap, “Nonlocal emergent hydrodynamics in a long-range quantum spin system,” *Phys. Rev. B* **101**, 020416 (2020).
- [76] Steven R. White and Richard L. Martin, “Ab initio quantum chemistry using the density matrix renormalization group,” *The Journal of Chemical Physics* **110**, 4127–4130 (1999).
- [77] Konrad Heinrich Marti and Markus Reiher, “The density matrix renormalization group algorithm in quantum chemistry,” *Zeitschrift für Physikalische Chemie* **224**, 583–599 (2010).
- [78] Sebastian Wouters and Dimitri Van Neck, “The density matrix renormalization group for ab initio quantum chemistry,” *The European Physical Journal D* **68** (2014), 10.1140/epjd/e2014-50500-1.
- [79] Takeshi Yanai, Yuki Kurashige, Wataru Mizukami, Jakub Chalupský, Tran Nguyen Lan, and Masaaki Saitow, “Density matrix renormalization group for ab initio calculations and associated dynamic correlation methods: A review of theory and applications,” *International Journal of Quantum Chemistry* **115**, 283–299 (2014).
- [80] Szilárd Szalay, Max Pfeffer, Valentin Murg, Gergely Barcza, Frank Verstraete, Reinhold Schneider, and Örs Leggeza, “Tensor product methods and entanglement optimization for ab initio quantum chemistry,” *International Journal of Quantum Chemistry* **115**, 1342–1391 (2015).
- [81] Huzihiro Araki, “Gibbs states of a one dimensional quantum lattice,” *Communications in Mathematical Physics* **14**, 120–157 (1969).
- [82] Yong Moon Park and Hyun Jae Yoo, “Uniqueness and clustering properties of gibbs states for classical and quantum unbounded spin systems,” *Journal of Statistical Physics* **80**, 223–271 (1995).
- [83] Michael M. Wolf, Frank Verstraete, Matthew B. Hastings, and J. Ignacio Cirac, “Area laws in quantum systems: Mutual information and correlations,” *Phys. Rev. Lett.* **100**, 070502 (2008).
- [84] M. Kliesch, C. Gogolin, M. J. Kastoryano, A. Riera, and J. Eisert, “Locality of temperature,” *Phys. Rev. X* **4**, 031019 (2014).
- [85] Andras Molnar, Norbert Schuch, Frank Verstraete, and J. Ignacio Cirac, “Approximating gibbs states of local hamiltonians efficiently with projected entangled pair states,” *Phys. Rev. B* **91**, 045138 (2015).
- [86] Tomotaka Kuwahara, Kohtaro Kato, and Fernando G. S. L. Brandão, “Clustering of conditional mutual information for quantum gibbs states above a threshold temperature,” (2019), [arXiv:1910.09425](https://arxiv.org/abs/1910.09425).
- [87] Ilya Kuprov, Nicola Wagner-Rundell, and P.J. Hore, “Polynomially scaling spin dynamics simulation algorithm based on adaptive state-space restriction,” *Journal of Magnetic Resonance* **189**, 241 – 250 (2007).
- [88] Alexander Karabanov, Ilya Kuprov, G. T. P. Charnock, Anniek van der Drift, Luke J. Edwards, and Walter Köckenberger, “On the accuracy of the state space restriction approximation for spin dynamics simulations,” *The Journal of Chemical Physics* **135**, 084106 (2011).
- [89] Tomaz Prosen, “Ruelle resonances in quantum many-body dynamics,” *Journal of Physics A: Mathematical and General* **35**, L737–L743 (2002).
- [90] Marko Ljubotina, Lenart Zadnik, and Tomaž Prosen, “Ballistic spin transport in a periodically driven integrable quantum system,” *Phys. Rev. Lett.* **122**, 150605 (2019).
- [91] Yichen Huang, C. Karrasch, and J. E. Moore, “Scaling of electrical and thermal conductivities in an almost integrable chain,” *Phys. Rev. B* **88**, 115126 (2013).
- [92] J. J. Mendoza-Arenas, S. R. Clark, and D. Jaksch, “Coexistence of energy diffusion and local thermalization in nonequilibrium xxz spin chains with integrability breaking,” *Phys. Rev. E* **91**, 042129 (2015).

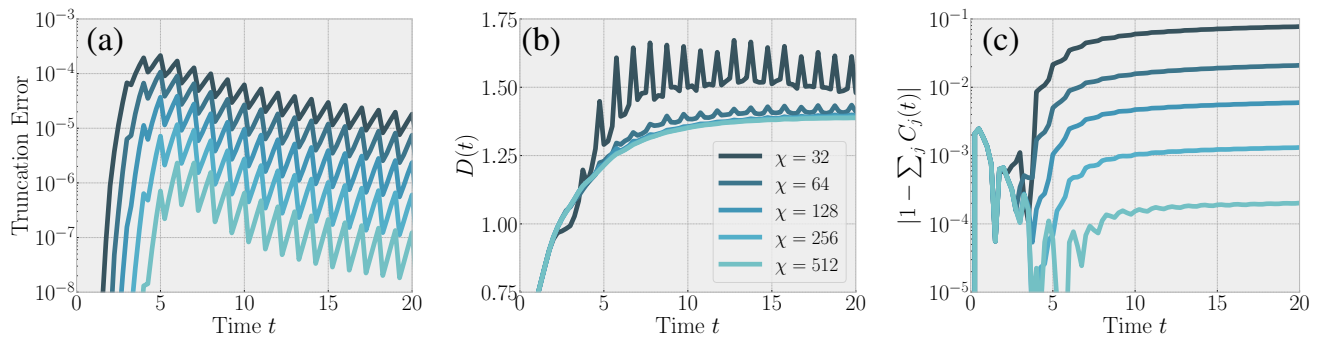


FIG. 4. Convergence of results with bond dimension χ in the Ising chain (4) for dissipation parameters $\ell_* = 4$, $\Delta t = 1$, $\gamma = 0.2$. (a): Truncation error per TEBD step, summed over all bonds in the chain ($L = 51$ sites). (b) Convergence of results for $D(t)$ (see main text for definition). (c) Errors in the energy conservation, as measured by the sum of the coefficients of local energy density terms $C_j(t)$.

Appendix A: Additional data for the Ising chain and XX ladder models

1. Convergence with bond dimension

In the main text, we showed that the dissipation leads to a decay of the operator entanglement at long times. Crucially, this makes the maximal operator entanglement encountered during the evolution independent of system size, depending only on the parameters of the dissipation. As we argued, we can therefore capture the diffusive spreading of correlations up to arbitrarily long times, without significant finite-size or truncation effects. Here we show explicitly how the curves for $D(t)$ converge as we increase the bond dimension χ .

The results are shown in Fig. 4 for the tilted field Ising model. We fix parameters $\ell_* = 4$, $\Delta t = 1$, $\gamma = 0.2$ (same as in Fig. 2(b)) and compare results for different bond dimensions $\chi = 32, 64, 128, 256, 512$. As the operator entanglement peaks and decreases (see Fig. 2(a)), the truncation error of the unitary TEBD time step also starts decreasing. While for small χ , the truncation errors encountered around the peak time are already significant, they decrease (roughly linearly) with χ . This also shows up in the results for the time-dependent diffusion constant, $D(t)$. While at small χ the truncation effects are clearly visible, the curves quickly converge as χ is increased.

Another way of testing the effects of truncation is by looking at whether the conservation law (in this case, of energy) is satisfied. We consider the correlations $C_j(t)$ and normalize them such that $\sum_j C_j(0) = 1$. The exact dissipative dynamics would maintain this normalization at all subsequent times due to energy conservation (assuming ℓ_* is larger than the support of the terms in the Hamiltonian, in this case $\ell_* \geq 2$). This is crucial for correctly capturing transport properties. We find that the errors in the conservation law, as measured by $|1 - \sum_j C_j(t)|$ quickly decrease as χ becomes larger. We conclude that it is possible to simulate the dissipative dynamics (2) up to long times, with a bond dimension that is independent of total system size.

2. Scaling collapse as a function of $\gamma/\Delta t$

Here, we justify our claim in the main text that when γ is sufficiently small, the results (in particular, estimates of D) are functions of the ratio $\gamma/\Delta t$ only. This can be seen by utilizing the Baker-Campbell-Hausdorff formula to rewrite the evolution operator (2) as

$$(\mathcal{D}_{\ell_*, \gamma} e^{i\mathcal{L}\Delta t})^N \equiv (e^{-\mathcal{K}_{\ell_*} \gamma} e^{i\mathcal{L}\Delta t})^N = \left(e^{-\mathcal{K}_{\ell_*} \gamma + i\mathcal{L}\Delta t + O(\gamma\Delta t)} \right)^N = e^{-\mathcal{K}_{\ell_*} N\gamma + i\mathcal{L}N\Delta t + O(\gamma N\Delta t)} = e^{t(i\mathcal{L} - \mathcal{K}_{\ell_*} \frac{\gamma}{\Delta t}) + O(\gamma t)}, \quad (\text{A1})$$

where $t = N\Delta t$ and we have introduced the logarithm of the dissipator, acting on a Pauli string as

$$\mathcal{K}_{\ell_*}[\mathcal{S}] = \begin{cases} 0 & \text{if } \ell_S \leq \ell_* \\ (\ell_S - \ell_*)\mathcal{S} & \text{otherwise.} \end{cases} \quad (\text{A2})$$

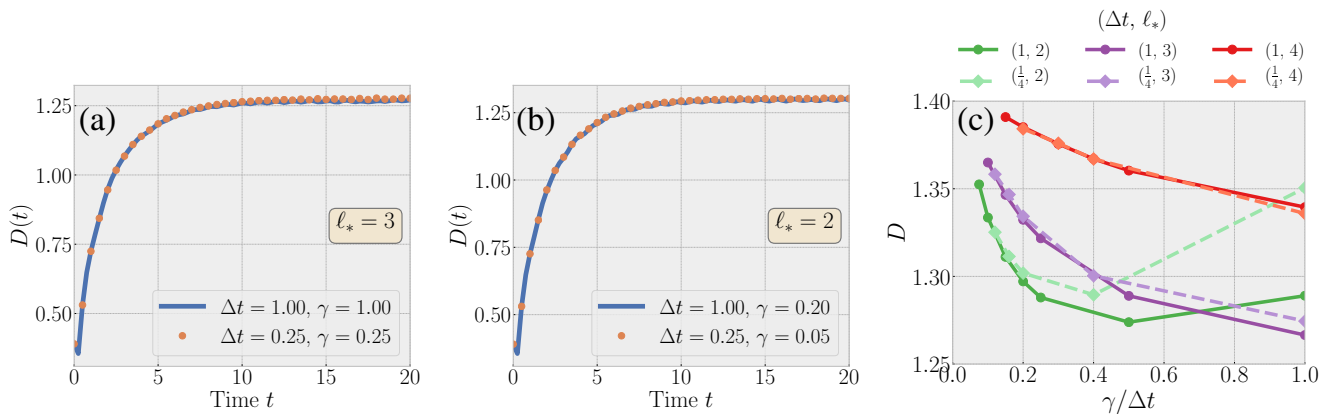


FIG. 5. Scaling collapse as a function of $\gamma/\Delta t$. (a,b): comparison of time-dependent diffusion constants for two curves with different Δt but the same ratio $\gamma/\Delta t$. When γ is sufficiently small, the results remain close to each other even at long times. (c): Estimates of $D \equiv \lim_{t \rightarrow \infty} D(t)$, comparing $\Delta t = 1$ and $\Delta t = 1/4$. In the small γ regime, relevant for extrapolation, the curves with the same ℓ_* collapse when plotted as function of $\gamma/\Delta t$.

In the second equality of Eq. (A1) we assumed $\gamma \ll 1$ to drop higher order terms that scale as $\gamma^2 \Delta t$. We also assume that Δt is at most an $O(1)$ quantity, so that terms that scale as $\gamma \Delta t^2$ are of the same order as $\gamma \Delta t$.

Eq. (A1) shows that the dynamics only depends on the ratio $\gamma/\Delta t$, and not on the individual value of γ and Δt , up to times $t \approx 1/\gamma$. As such, it does not directly constrain the diffusion constant, which is extracted from the long-time limit. However, in practice we find that $D(t)$ saturates to a constant at a finite time t_{sat} . While t_{sat} itself depends on γ and Δt (as well as on the Hamiltonian), we find that this dependence is relatively weak; in particular, t_{sat} should converge to a finite, $O(1)$ value as $\gamma \rightarrow 0$. Therefore, estimate of D should also depend only on the ratio $\gamma/\Delta t$, provided that we are in the regime where $\gamma t_{\text{sat}} \lesssim 1$.

Testing this expectation on the Ising chain (4), we find that it works remarkably well, even for $\gamma \approx 1$ (we also find that it works increasingly well as ℓ_* gets larger). This is shown in Fig. 5. Figs. 5(a,b) show that curves with identical ratio $\gamma/\Delta t$ are the same at early times, and, moreover, their late time saturation values are also close to one another, provided that we are in a regime with sufficiently small γ . Consequently, the estimates for D show a scaling collapse when data for the same ℓ_* but different Δt , are plotted as a function of $\gamma/\Delta t$, see Fig. 5(c).

3. Operator weights

In the main text, we noted that the operator von Neumann entropy of the dissipatively evolving local density approaches 1 (in units of $\ln 2$) at long times. This suggests a long-time behavior where the evolving operator is increasingly dominated by its diffusive, ‘conserved’ part, $\tilde{q}_0(t) \approx \sum_j C_j(t) q_j$. We now further support this interpretation by calculating the weight of various operators in \tilde{q}_0 (in this section we use a different notation from the main text, with 0 denoting the center site).

To define what we mean by the weight of an operator, let us expand \tilde{q}_0 in the basis of Pauli strings, $\tilde{q}_0 = \sum_{\mathcal{S}} c_{\mathcal{S}}(t) \mathcal{S}$; the weight of the Pauli string is then the squared coefficient, $|c_{\mathcal{S}}|^2$. The total weight on operators with length ℓ is given by

$$W_{\ell}(t) \equiv \sum_{\substack{\mathcal{S} \\ \ell_{\mathcal{S}} = \ell}} |c_{\mathcal{S}}(t)|^2. \quad (\text{A3})$$

For unitary evolution one would have a conserved total weight, $\sum_{\mathcal{S}} |c_{\mathcal{S}}(t)|^2 = \sum_{\ell} W_{\ell}(t) = 1$. During evolution, the weight gets redistributed from short operators to an essentially random superposition of long ones, such that at time t the operator is dominated by strings of length $\ell \sim v_{\text{B}} t$, with v_{B} the butterfly velocity. This leads to the linear growth of operator entanglement with time.

The dissipator fundamentally changes this picture, as it *removes* operator weight from long strings. This reverses the effect of the unitary dynamics, making the contribution of short operators dominant at long times, which leads to the observed decay in the entanglement. While short operators, with $\ell \leq \ell_*$, are not affected directly by the dissipator,

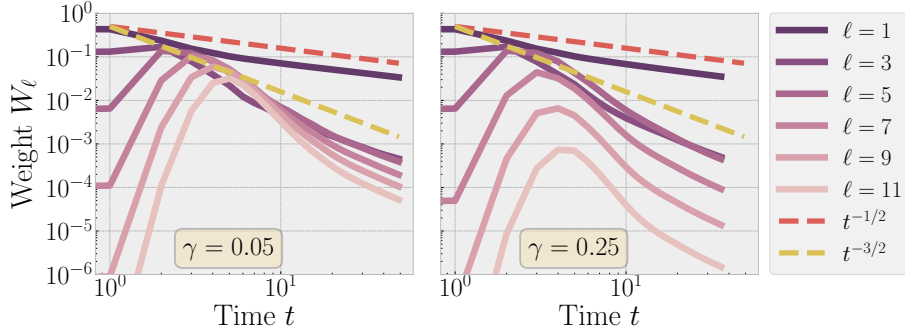


FIG. 6. Total weight on strings of size ℓ as a function of time. The majority of the remaining (not yet dissipated) weight is on 1-site strings as decays as $t^{-1/2}$. The weight of longer strings decays as $t^{-3/2}$. Data shown for $\Delta t = 1$, $\ell_* = 5$ with $\gamma = 0.05$ (left) and $\gamma = 0.25$ (right).

their weight also decreases as they get converted into longer strings which are subsequently dissipated. However, due to the hydrodynamic nature of transport, we find that the weight associated to local densities, $|C_j|^2 \equiv |c_{q_j}|^2$ decreases parametrically more slowly than those of non-conserved operators, so that they dominate at long times.

To show this, we consider the XX ladder (5) and consider the evolution of the spin density, $\tilde{Z}_0(t)$. Calculating operator weights for this object, we find that the weight on local densities decays as $W_{\ell=1} \sim t^{-1/2}$, as expected from the diffusive nature of spin transport [31, 32]. Considering larger ℓ , we find two things. First, for $\ell > \ell_*$, the weight decreases exponentially with ℓ , as expected from the form of the dissipator. More importantly for the present discussion, we also find that the weights for $\ell > 1$ decay parametrically faster in time, $W_{\ell>1} \sim t^{-3/2}$ (even when $1 < \ell \leq \ell_*$); this is shown in Fig. 6.

This behavior is consistent with the operator spreading picture developed in Refs. 31 and 32. In this picture, one rewrites the time evolved density $q_0(t)$ as

$$q_0(t) = q_0^D(t) + q_0^B(t) \quad (\text{A4})$$

where $q_0^D(t) \equiv \sum_x C(x,t)q_x$ is the diffusive part of the operator and we assume that $C(x,t) \equiv \langle q_x | q_0(t) \rangle$ is well approximated by an unbiased diffusion kernel. $q_0^B(t)$ contains the contributions from all remaining Pauli strings, and is dominated by those with length $\ell = 2v_B t$, with v_B the operator butterfly velocity [29, 30]. The unitary dynamics leads to a conversion of weight from the diffusive to the ballistic part, whose local rate is given by ‘current’ squared, $|\partial_x C(x,t)|^2$. In this way, at each time step q_0^D sources new ballistically growing operators which thereafter form part of q_0^B . This picture can be used to deduce the behaviour of W_ℓ as a function of time. According to the above picture, operators of support ℓ would correspond to terms in q_0^B which have been ballistically growing for a time interval $t - \tau = \ell/(2v_B)$. The weight of such terms is therefore expected to be

$$\int dx (\partial_x C(x,\tau))^2 \sim \left[D \left(t - \frac{\ell}{2v_B} \right) \right]^{-3/2}.$$

This shows that the weight on length ℓ operators at time $t \gg \frac{\ell}{2v_B}$ goes as $(Dt)^{-3/2}$.

Appendix B: Spin diffusion in Floquet circuits

We now complement the results shown for energy-conserving, Hamiltonian dynamics in the main text, with data on time-periodic models. We construct these as circuits of local unitary gates, with a ‘brick-wall’ structure and consequently, a strict light cone. This structure is illustrated in Fig. 7(a). We use the same two-site unitary u in each gate, such that the system has translation invariance in space (with unit cells composed of two sites) and in time (by two layers of the circuit).

We want our circuit to conserve the total spin- z component. For a spin-1/2 chain, such a circuit is fully parametrized by three numbers, and it corresponds to a Trotterized version of an XXZ chain with a staggered magnetic field

$$u = e^{-i(J_{xy}(S_1^x S_2^x + S_1^y S_2^y) + J_{zz} S_1^z S_2^z + g(S_1^z - S_2^z))}, \quad (\text{B1})$$

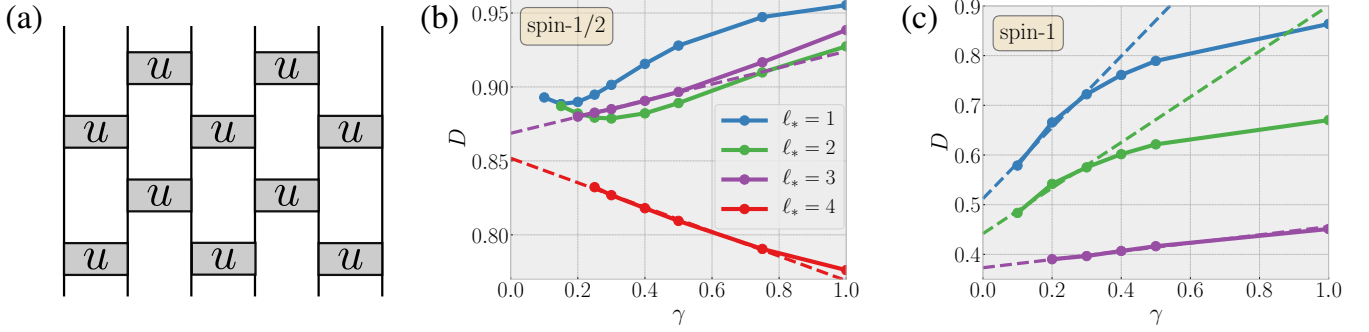


FIG. 7. Diffusion constants in Floquet circuits. (a) The circuits have a brick-wall structure, updating even/odd bonds in turn. Every gate is given by the same S_z -conserving two-site unitary u . (b,c) Estimates of the spin diffusion constant for the circuit defined by Eq. (B1), for spin-1/2 and spin-1 chains.

where we have now used spin operator S^α instead of Pauli matrices (the two differ by a factor of 2), and the subscripts refer to the two sites on which the gate acts. We choose irrational values of the three couplings, $J_{xy} = 2\sqrt{7}$, $J_{zz} = 2\sqrt{5}$, $g = 2\sqrt{3}$.

We apply our dissipative evolution method for this circuit model, applying the dissipator after every second layer of the circuit (i.e., one Floquet period). We extract spin diffusion constant in the same way as in the main text. The results for the spin-1/2 circuit are plotted in Fig. 7(b). We find that the convergence to $\gamma = 0$ is less clear than in the Hamiltonian models we studied in the main text. In particular, for $l_* = 1, 2$ we observe a strong non-monotonicity with γ , while $l_* = 3, 4$ do appear to converge linearly to compatible values of D . Nevertheless, we note that the variations in D are all relatively small.

Our interpretation is that the apparent lack of convergence in Fig. 7(b) is not related to the Floquet circuit nature of our model; rather, it has to do with the fact that it is close to an integrable point. It was recently shown [90] that for $g = 0$, the model in Eq. (B1) is integrable; this is closely related to the integrability of the XXZ Hamiltonian. In the latter case, a staggered field is known to break integrability [62, 91, 92], so we expect that for generic g our circuit is also non-integrable. However, we believe that the nearby integrable point is responsible for the non-trivial behavior we observe (for example some almost-conserved operator of length $\ell = 3$ could explain why the $l_* \leq 2$ curves have a qualitatively different behavior from $l_* \geq 3$).

To test this intuition, we also consider the spin-1 version of the same model. That is, we use the same definition of the two-site gate as in Eq. (B1), but with $S_{1,2}^\alpha$ standing for spin-1 operators. The results for this case are shown in Fig. 7(c). While we find that getting to smaller γ becomes quite difficult in this case, due to a quick initial growth of operator entanglement, so that our results are not as precisely converged as for the models presented in the main text, we find no evidence of strong non-monotonicities in the regime we can simulate. This reinforces our belief that the peculiar behavior exhibited by the spin-1/2 model is tied to the presence of nearby integrable points.